NONLINEAR OSCILLATION AND CHAOTIC MOTION OF A VEHICLE SUSPENDED BY PERMANENT MAGNETS IN REPULSION

Emil H. Gad
Mechanical Engineering Department, Faculty of Engineering,
Zagazig University, Zagazig, Egypt.

ABSTRACT

The nonlinear oscillations of a passively levitated vehicle, which is assumed to be moved in a vertical direction and suspended by the magnetic repulsive force of a moving guideway, are analyzed numerically and a computer program is developed. The objective of this paper is to point out the effects of the nonlinearity of the magnetic lift force on the oscillations of the vehicle. The spring force is typical of an asymmetrical soft spring and the large amplitude free vibration resembles a hopping motion. Harmonic vibration appears throughout the frequency range and ½ subharmonic vibration occurs in the unstable region of the harmonic vibration when the exciting frequency is approximately twice the linear natural frequency. For a suitable combination of parameters (damping, exciting amplitude and exciting frequency), many successive bifurcations of doubling period as well as aperiodic vibrations are observed. The aperiodic vibration is identified as chaotic vibration by applying the frequency spectrum, the Lyapunov exponent, the strange attractors and the invariant manifold inspections.

Key words: Magnetic Levitation, Simulation, Nonlinear Vibration, Chaos, Bifurcation, Harmonic Vibration, Subharmonic Vibration, Lyapunov Exponent, Strange Attractor, Aperiodic Vibration.

1. INTRODUCTION

In the conventional study of random vibrations, one usually assumes the existence of some random input, either in the applied external force or in the parameters of the dynamical system [1]. In the last few years, researchers in a number of different fields have obtained solutions to deterministic differential equations, through simulation, which exhibit chaos-like random vibration. Chaotic dynamics in deterministic systems has established itself as a new phenomenon in nonlinear vibrations. Chaotic vibrations can occur in systems when strong nonlinearities exist such as rotor-ball bearing system [2], synchronous periodic and chaotic systems [3], a system having an asymmetrical spring [4] and magnetic levitation system [5].

The phenomenon of magnetic levitation (Maglev) has fascinated philosophers through the ages. In recent time, it has attracted much attention from scientists and engineers as a mean of eliminating friction or physical contact. Although the area of frictionless bearings is important, it is the application of contactless suspension and levitation to high-speed ground transportation. Regardless of the method employed, the vehicles are described as "Hover Trains" or "Maglev Train". There are many experiments for preparation and operation of a superfast Maglev train. It will be able to fly along at a maximum speed of 550 Km/hr, while levitated by a magnetic force induced by magnets. Maglev train does not float while starting up or slowing down, but uses tires in the same way as an airplane. A schematic section of the Maglev vehicle and guideway is shown in Figure (1) [6]. Recent developments in fabricating permanent magnets from high coercivity ferrite materials have once again raised interest in the idea of using such magnets for levitation of vehicles. Polgreen in 1968 was the first to propose an application in the form of a vehicle [7].

In this paper, the developed computer program is used to numerically examine the nonlinear oscillations of the magnetically levitated vehicle.

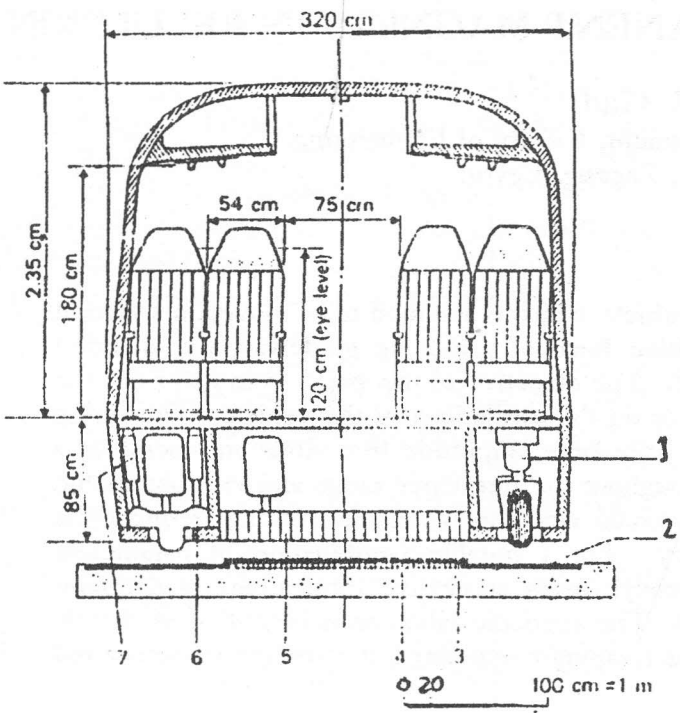

1. Retractable wheel for low speed suspension
2. Magnetic guideway surface for levitation
3. Guideway.
4. Linear synchronous motor windings
5. Propulsion magnet
6. Levitation magnet
7. Secondary suspension

Figure 1. A schematic section of the magnetic levitation vehicle and guideway [2].

The vehicle has many degrees of freedom. Simplifying, the guideway is assumed to oscillate sinusoidally in the vertical direction. For the magnetically levited vehicle which can be moved freely in the vertical direction, the mechanism of the excitation is shown in the case when the guideway is oscillated in the neighborhood of twice the natural frequency of the oscillation [8]. Furthermore, various oscillations have been noted to occur owing to the periodic change of the lift force which acts on the repulsive-type magnetically levitated vehicle moving on a guideway. For suitable combination of parameters (damping, exciting amplitude and exciting frequency), many successive bifurcations of doubling period as well as aperiodic vibrations are observed. The aperiodic vibration is identified as chaotic using diagnostic tools [9-12] as: phase plane history, Fourier spectrum, Poincaré maps, Feigenbaum number, bifurcation diagrams and Lyapunov exponents.

2. EQUATION OF MOTION

The dynamic behavior of the system is analyzed, in which a vehicle moves with light damping under the influence of a nonlinear spring force. The vehicle is symmetrical, on which the magnetic lift force symmetrically acts about the vertical axis in the static equilibrium state. A dynamical model of the levitated vehicle moving as a single- degree -of-freedom system is presented in Figure (2). The length of the magnet which is fixed on the guideway is assumed to be sufficiently large compared with the length of the magnet of the vehicle. The gap length between the magnets of the vehicle and the guideway is assumed z. These magnets repulse each other with the same magnetic poles, and the guideway is excited sinusoidally in the vertical direction.

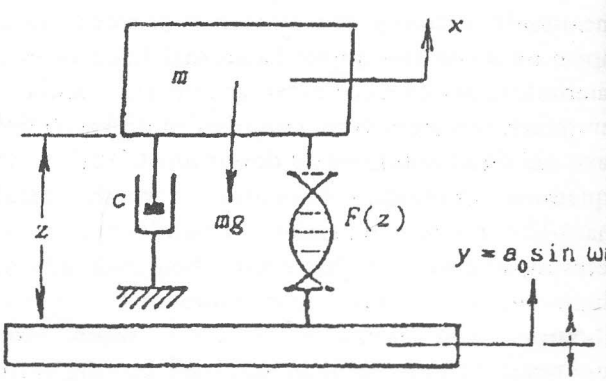

Figure 2. Modelling of the system.

The system possesses a nonlinear unsymmetrical spring function composed of a magnetic repulsion under gravitational force. The magnetic force is assumed to be proportional to the reciprocal of square of pole gap length, which may be valid in principle for non-active magnetic levitation. The

nonlinearties is assumed to be arise only from the magnetic lifting force and that the dissipative force acting on the system is linear, the equation of motion is

$$m\frac{d^2x}{dt^2}+c\frac{dx}{dt}+F(z)=-mg \qquad (1)$$

where m is the mass of levitated vehicle, x is the displacement of vehicle (vs. absolute frame), t is time, c is the linearized damping coefficient,

$$F(z) = -B/(1+\beta z)^2 \qquad (2)$$

is the magnetic repulsive force [13], B and β are constants (> 0),

$$z = x - a_o \sin \omega t \qquad (3)$$

is the gap length between pole faces (> 0), a_o and ω are the amplitude and frequency of the guideway excitation respectively, and mg is the gravitational force.

Upon the introduction of the nondimensional quantities

$$\eta = [x-(z_o + a_o \sin \omega t)] / x_o,$$

$$\theta = [\omega t - \tan^{-1}(\gamma/u)]/u, \qquad (4)$$

in which;

$$\gamma = c/m\omega_n,\quad u = \omega/\omega_n,$$

$$z_o = \left(\sqrt{B/mg}-1\right)/\beta,\quad x_o = \sqrt{B/mg}/\beta, \qquad (5)$$

where η is the nondimensional displacement, z_o is the equilibrium gap length, θ is the time scale, x_o is the equilibrium distance, γ is the damping factor, u is the frequency ratio, and

$$\omega_n = \sqrt{2\beta g^{\frac{3}{2}}\sqrt{m/B}}; \qquad (6)$$

is the asymptotic linear ($z \to z_o$), natural frequency, equation (1) can be reduced to the following nondimensional equation of motion

$$\frac{d^2\eta}{d\theta^2}+\gamma\frac{d\eta}{d\theta}+\varphi(\eta)=P\sin u\theta \qquad (7)$$

in which ;

$$\varphi(\eta)=\frac{1}{2}\left[1-\frac{1}{(1+\eta)^2}\right] \qquad (8)$$

$$P = au\sqrt{u^2+\gamma^2},\quad a = a_o / x_o$$

where $\varphi(\eta)$ is the nonlinear spring function, P is the exciting amplitude, and a is the nondimensional amplitude.

3. SPRING FUNCTION AND FREE VIBRATION

The nonlinear spring function $\varphi(\eta)$ of the magnets is

$$\varphi(\eta) = [1-1/(1+\eta)^2]/2 = (1+\eta/2)\,\eta/(1+\eta)^2 \qquad (9)$$

where η is the nondimensional displacement. The spring function is illustrated in Figure (3) (solid line). It posses the property of strongly nonlinear with unsymmetrical soft spring which has the unit rigidity at the origin and is pounded in displacement as well as in restoring force. The limits of the force pattern $\varphi(\eta)$ for the displacement η as shown in Figure (3) are

$$-1 < \eta < \infty,\ -\infty < \varphi(\eta) < 1/2,$$

$$\lim_{\eta \to -1+} \varphi(\eta) = -\infty +,$$

$$\lim_{\eta \to \infty-} \varphi(\eta) = 0.5 - \quad \text{(broken line)}, \qquad (10)$$

the slope at the origin ;

$$d\varphi(\eta)/d\eta\,|_{\eta=0} = 1 \quad \text{(dotted line)}.$$

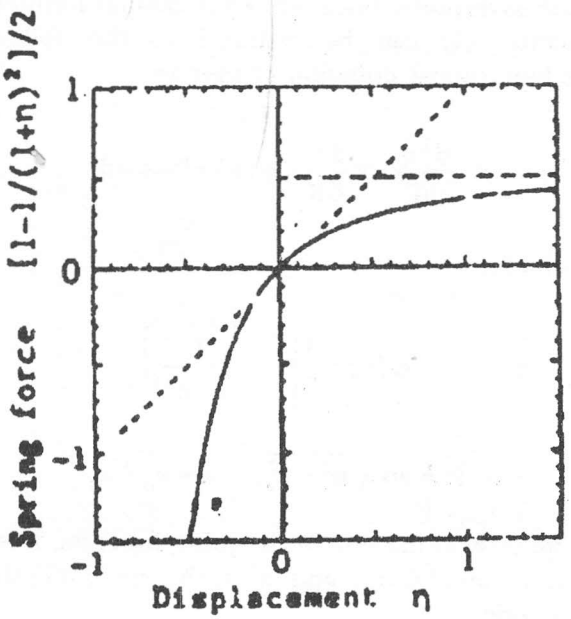

Figure 3. Spring property.

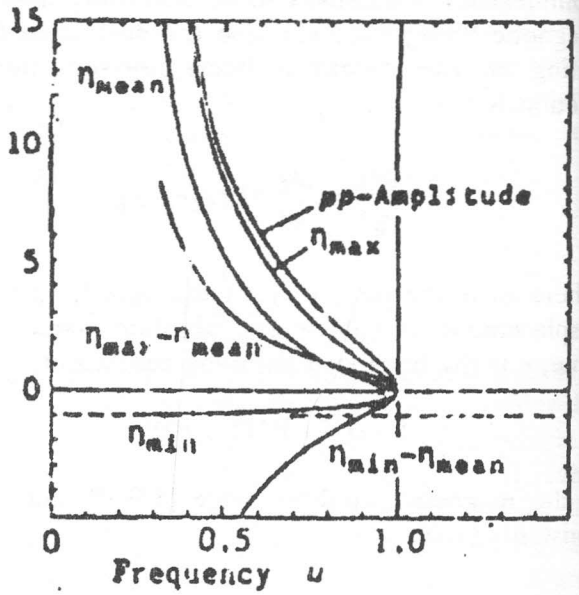

Figure 4. Frequency response of the free vibration

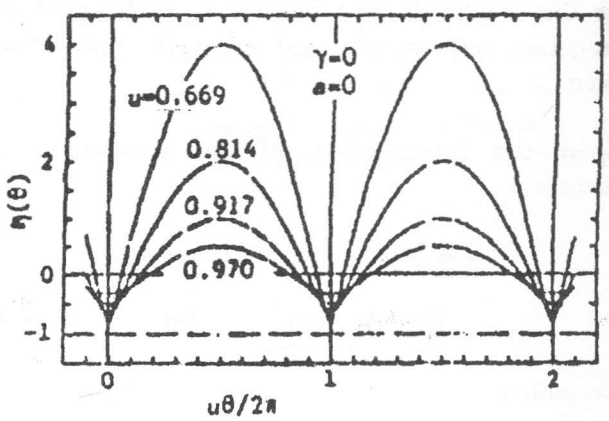

Figure 5. Wave-form of the free vibration.

Since nonlinear term is involved in equation (7), no analytical method can be directly applied, but numerical method is applied. A computer program for solving the differential equation (7) is developed using Runge-Kutta-Gill (RKG) method with shooting technique [14] to capture a desired subharmonic motion by iterating on the initial conditions.

The equation of motion of the free vibration, i.e. for $\gamma = 0$ and $P = 0$ in equation (7), is

$$\frac{d^2\eta}{d\theta^2} + \frac{1}{2}\left[1 - \frac{1}{(1+\eta)^2}\right] = 0 \qquad (11)$$

The computations of the free vibration were carried out and the peak-to-peak amplitude (PP-Amplitude) versus the frequency is plotted in Figure (4). Frequency responses of amplitudes ; $\eta_{max.}$, $\eta_{min.}$, η_{mean}, $\eta_{max.} - \eta_{mean}$ and $\eta_{min.} - \eta_{mean}$, for the free vibration are also shown in Figure (4). Wave forms for several amplitudes (Frequencies; u = 0.669, 0.814, 0.917 and 0.970), are shown in Figure (5).

4. EXCITED STEADY VIBRATIONS (HARMONIC AND SUBHARMONIC RESPONSES)

The numerical results of the PP-Amplitude as a function of the frequency ratio u is plotted in Figure (6) for combinations of the system parameters; damping factor ($\gamma = 0.1$ and 0.2), and excitation force nondimensional amplitude ($a = 0.1$ and 0.4). In figure (6), the stable solutions are presented by solid lines while the unstable solutions are shown by dotted lines. The small circles show the boundary between the stable and unstable states. Associated

numbers indicate the order of synchronization; "1" for "harmonic response" and "1/2, 1/3, 1/4" for "Subharmonic response". The response curves corresponding to fractions of order greater than 4 and those of the successive period doubling are omitted for simplicity. Harmonic response converges to zero for $u \to 0$ and to 0.2 for $u \to \infty$. In the vicinity of u~2 it loses the stability and the strong 1/2 subharmonic occurs exactly over the unstable harmonic region.

The effects of varying the damping ratio; $\gamma = 0.1$ and 0.2, where the exciting amplitude is held constant, are shown in Figure (6a,b) for $a = 0.1$, and in Figure (6c,d) for $a = 0.4$. The effects of varying the excitation amplitudes; $a = 0.1$ and 0.4, where the damping ratio is held constant, are shown in Figure (6b,d) for $\gamma = 0.1$, and in Figure (6a,c) for $\gamma = 0.2$. The figure shows clearly that higher damping suppresses the higher order subharmonic responses. The subharmonics 1/2, 1/3, and 1/4 are presented for the following combinations of the damping factor and exciting amplitude; ($\gamma = 0.1$, $a = 0.1$), ($\gamma = 0.2$, $a=0.4$), and ($\gamma = 0.1$, $a = 0.4$), in Figure (6b,c and d) respectively while the harmonic response was observed in the previous combinations in addition to ($\gamma = 0.2$, $a = 0.1$), as shown in Figure (6a) in which the subharmonic are not exists.

5. PERIOD DOUBLING AND BIFURCATIONS

When the frequency u is slowly changed, the period-doubling starts from the boundary between stable/unstable response curves and it bifurcates into successive period-doubling. The period-doubling or flip bifurcations did not occur in a narrow range of u. The bifurcation diagram is shown in Figure (7), which indicates the Poincaré points of displacement i.e., η ($u\theta = 2\pi$ x integer) vs. frequency u. The damping factor $\gamma = 0.2$ is constant and the nondimensional excitation amplitude a is gradually increased, so that $a = 0.12 \sim 0.40$, while the frequency is swept down from $u = 3.0$ to 1.0, except for $a = 0.40$, also the frequency is swept up from u=1.0 to 3.0 by step size 0.005.

Two types of period-doubling bifurcations are observed. For the moderate level of excitation; a=0.12 ~ 0.36, a finite number of period-doubling bifurcations were found. For the high level of excitation; $a = 0.37 \sim 0.40$, chaotic motions occurred through an infinite number of period-doubling bifurcations. In figure, discrete lines corresponding to a value of u imply the steady vibration (harmonic and subharmonic), and random points to chaotic motion.

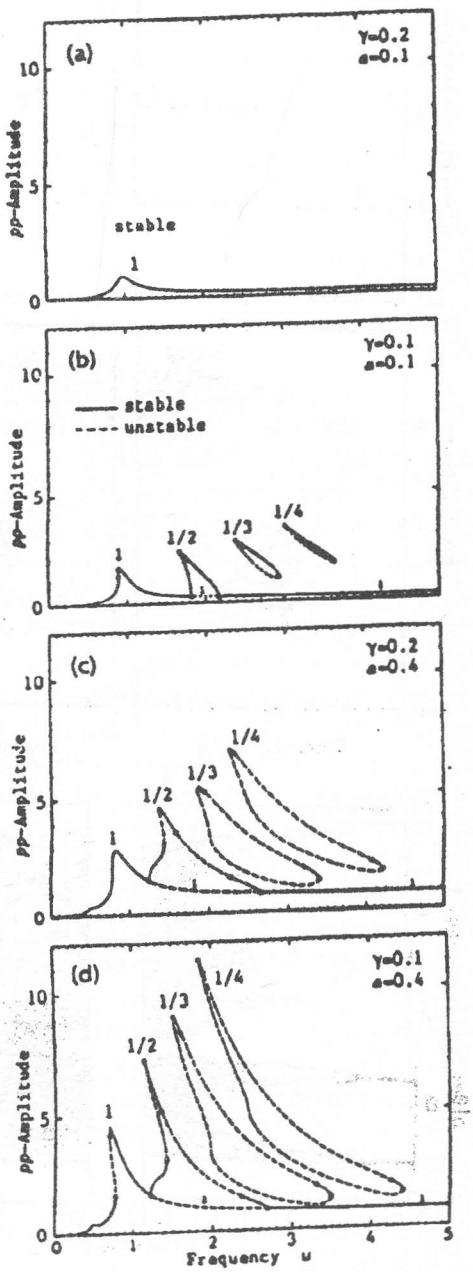

Figure 6. Frequency response of the steady state vibration (harmonic/subharmonic vibration).

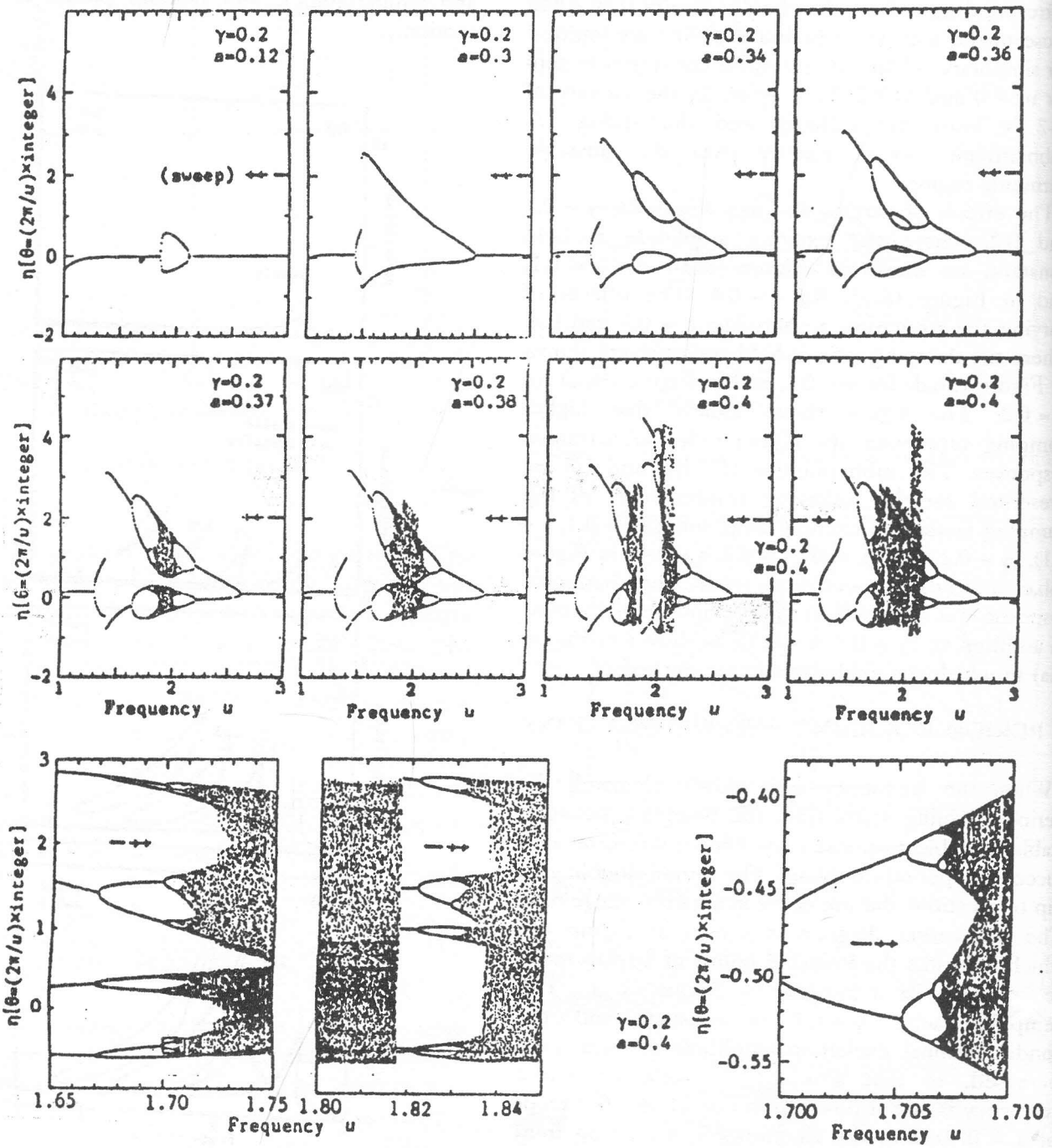

Figure 7. Bifurcation diagram.

The response curves in the regions of u = 1.65 ~ 1.75, u = 1.80 ~ 1.85 and u = 1.700 ~ 1.710 for the case of γ = 0.2 and a = 0.4 are magnified in the three lower diagrams of Figure (7). A series of

bifurcations is found such that a harmonic vibration changes into subharmonics of order ½, ¼, and 1/8 successively and so on. They occur in such a manner that the subharmonic of order ½ appear first in the region of the unstable harmonic one, that of order ¼ next in the region where the ½ subharmonics turn unstable, and that of order 1/8 appears where the one of ¼ becomes unstable, and so on.

Figure (8) shows the waveform/Lissajous-figure of the velocity/displacement in the bifurcation process. The figure shows that a harmonic response exists for u = 1.2470, while for u = 1.2473, the 1/2 subharmonic oscillation exists. As u increases, higher order subharmonics; 1/2, 1/4 and 1/8 are observed. When the frequency is swept down, a harmonic oscillation exists for u =5 .0, while for u = 2.6560 the 1/2 subharmonic oscillation is observed. As u decreases, higher order subharmonics; 1/2, 1/4, and 1/8 will take place. Finally it reaches the chaotic motion at the middle of the unstable zone according to the fine change of the frequency from both fringes of the zone towards the interior.

Frequency values which correspond to successive bifurcations (see Table (1)), satisfy fairly well the Feigenbaum relation

$$\delta_i = \frac{u_i - u_{i-1}}{u_{i+1} - u_i} \qquad (12)$$

where u_n is the transition frequency from 2^n-period solution to 2^{n+1}-period solution. For further increase of u, the period-two orbit becomes unstable and a period-four cycle emerges only to bifurcate to a period-eight cycle for a higher value of u. This period-doubling process continues until u approaches the values u_∞ = 3.56994 ..... Near this value, the sequence of period-doubling parameter values scales according to a precise law:

$$\lim_{i\to\infty} \delta_i = 4.66920...$$

The limit ratio is called the "Feigenbaum number" [15].

6. NONPERIODIC MOTION AND CHAOS

Chaotic motions are detected by direct numerical integration and stability analysis in a narrow frequency zone. The nonperiodic motion is understood to be a chaos by applying diagnostic tools as: Fourier spectrum, Poincaré mapping and Lyapunov exponents. One of the clues for detecting chaotic vibrations is the appearance of a broad spectrum of frequencies in the output when the input is a single-frequency harmonic motion. Examples of FFT analysis, are shown in Figure (9), for the case of γ = 0.2 and a= 0.4. In Figure (9) (a), Fourier spectrum is shown for the case of chaotic oscillation at the frequency u = 2.0. It exhibits continuous spectra except at the frequency of the harmonic excitation synchronized with the frequency component and its higher multiple components where line spectra are generated. The oscillation may therefore be confirmed to be a nonstationary oscillation composed of uncountable frequency components.

On the other hand, spectra for the case u = 2.02 and 2.375 shown in Figures (9b) and (9c) , are presumed to be nearly periodic oscillations. They are composed of many discrete line spectra corresponding with the frequency component of the harmonic oscillation and its higher harmonics, and many additional secondary components. The minor appearance of continuous spectra is considered to be due to noise, e.g., perhaps caused by unsuitable window processing. The results show the oscillation to be a nearly periodic oscillation which must produce essentially discrete line spectra.

The Poincaré mapping in the phase plane composed of displacement vs. velocity is shown in Figure (10) for the case of γ = 0.2 and a = 0.4, which exhibits the chaotic attractor. The figure shows an attractor for some frequencies u = 1.8, 1.9 and 2.0, which corresponds to nonstationary oscillations. They seem quite complicated, but the zone attractor is seen in the vicinity of the unstable periodic solution, and then they may be considered strange attractors which represent characteristically the salient features of the chaos. The invariant manifold also shows evidence of the chaotic phenomena, i.e., the existence of the homoclinic points.

The Lyapunov exponent, is computed and the results are shown in Figure (11), which are accompanied by some bifurcation diagrams (see Figure (7)), for reference. One of the Laypunov exponents is positive which verifies the existence of chaotic motions. The spectrum of Lyapunov exponents at u = 2.0 is 0.01, 0.0, -0.03. The Lyapunov exponents test the sensitivity of the system response to changes in the initial conditions.

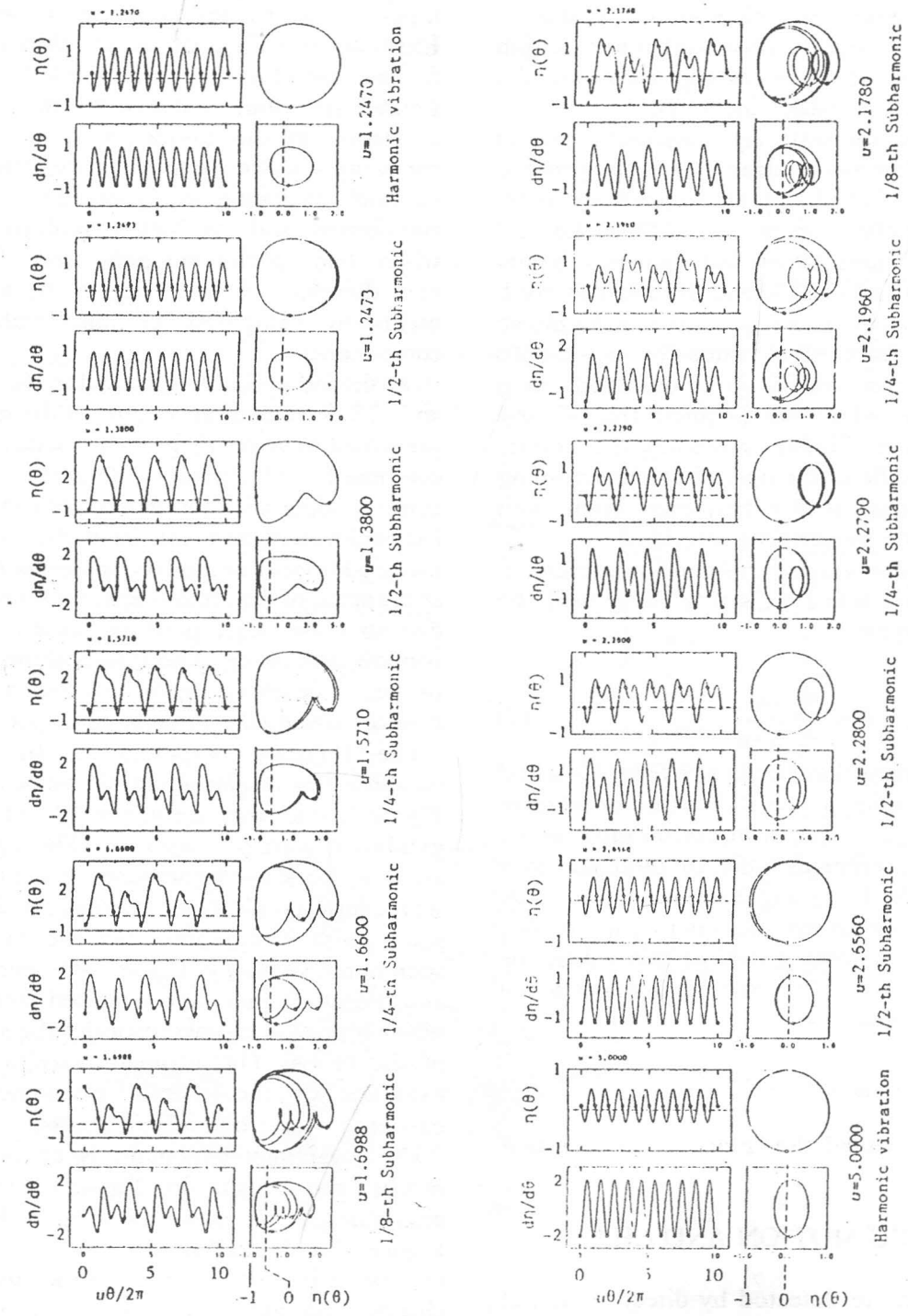

Fig. 8 Wave-form/Lissajous-figure of the velocity/displacement in the bifurcation process.

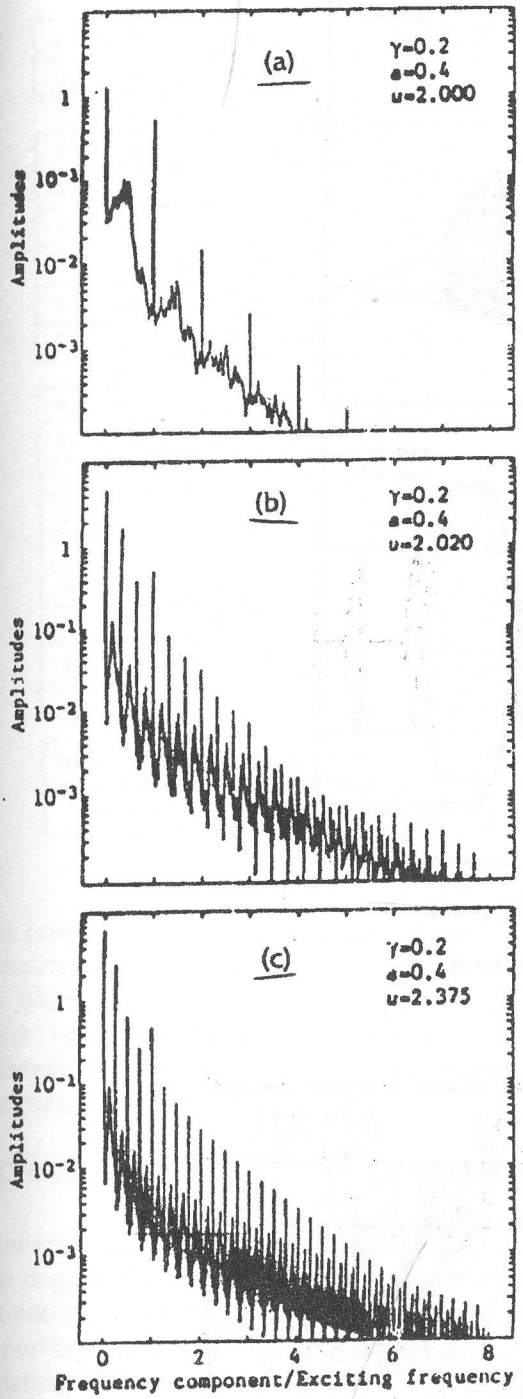

Figure 9. Fourier spectrum.

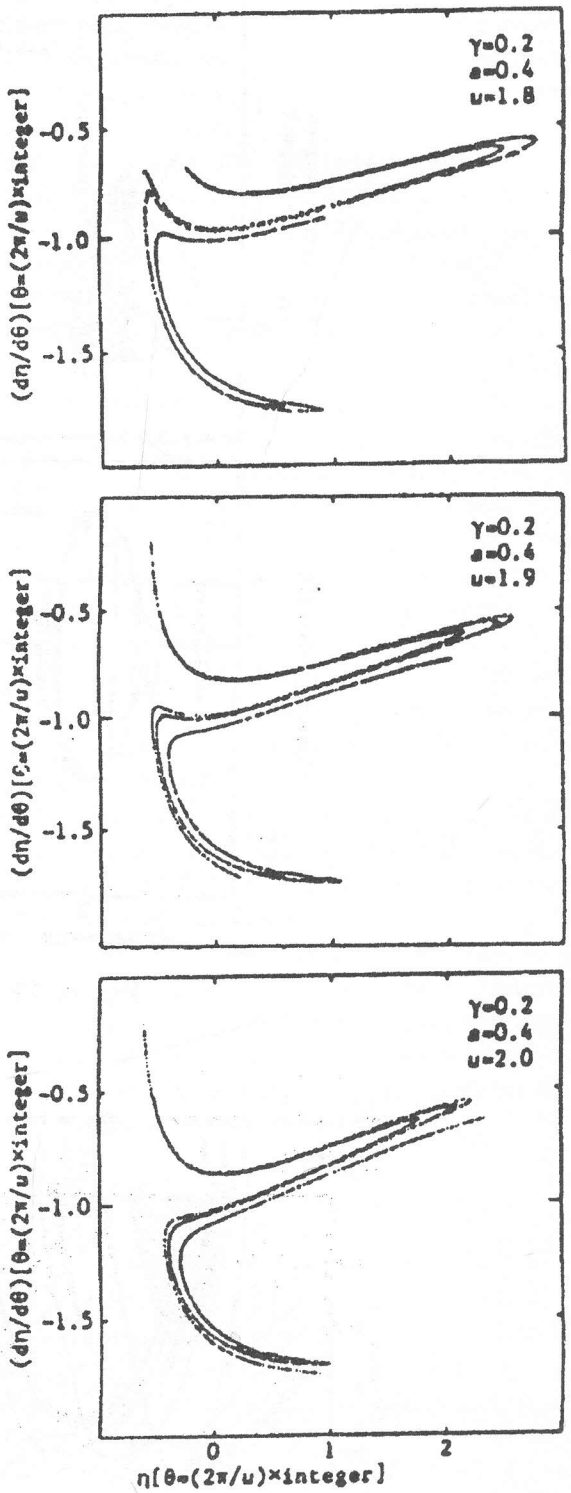

Figure 10. Poincaré map.

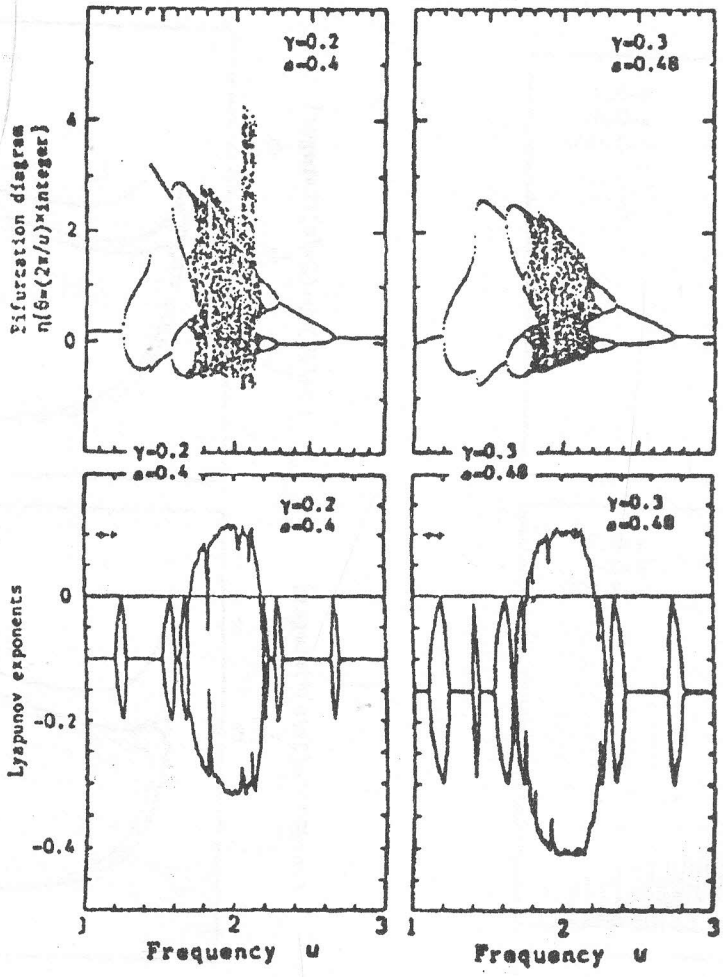

Figure 11. Lyapunov exponent.

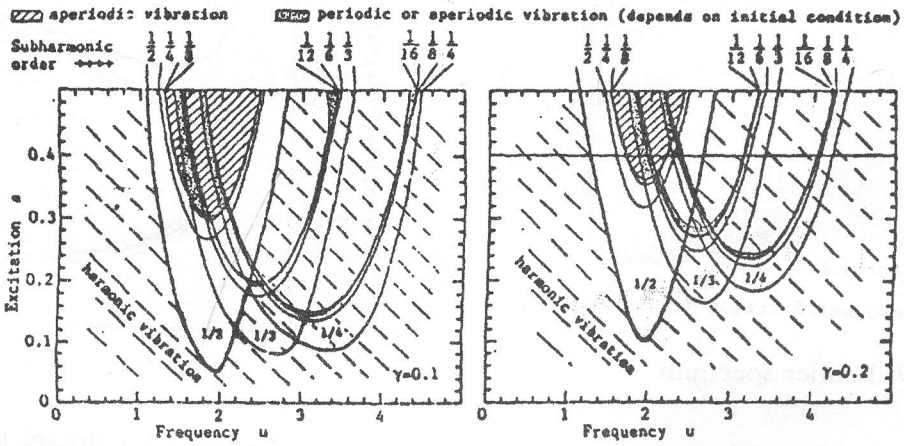

Figure 12. Chaos diagram.

Table 1. Feigenbaum number.

n	period	u_n	δ_{n-1}
0	1	1.247253860	——
1	2	1.570294086	——
2	4	1.669660488	3.250099
3	8	1.698840392	3.404603
4	16	1.705278847	4.538841
5	32	1.706659113	4.651293
6	64	1.706955387	4.666174
7	128	1.707018851	4.668379

n	period	u_n	f_{n-1}
0	1	2.658816458	——
1	2	2.279690696	——
2	4	2.195509235	4.479915
3	8	2.177252909	4.811084
4	16	2.173182051	4.495662
5	32	2.172312120	4.614873
6	64	2.172123085	4.654658
7	128	2.172082571	4.665918

Note; $\delta_n=(u_n-u_{n-1})/(u_{n+1}-u_n)$, where u_n: transition frequency from 2^n-period-solution to 2^{n+1}-period-solution

The total vibratory characteristics of the system is summarized as a "chaos diagram" shown in Figure (12), which indicated the occurrence regions of several types of vibration including; harmonic, subharmonic and chaos, drawn in a parameter plane of frequency and amplitude of the excitation.

7. CONCLUSIONS

Nonlinear oscillation of a dynamical system with single-degree-of-freedom, which contains nonlinear magnetic repulsive force between levitated vehicle and moving guideway, is analyzed using computer simulation. From the numerical results the following conclusions are drawn:

1. The spring function of the magnet possesses the property of strongly nonlinear with unsymmetrical/soft spring and the large amplitude free vibration resembles a hopping motion.
2. Harmonic vibration appears at all the range of frequency and the subharmonic vibration occurs on the unstable region of harmonic vibration.
3. As the excitation amplitude increases higher order subharmonic oscillations are observed. One characteristic precursor to chaotic motion is the appearance of subharmonic periodic vibration.
4. Two types of period-doubling bifurcations route to chaos were observed. For the moderate level of excitation amplitude, a finite number of period-doubling bifurcations were found, while for the high level of excitation amplitude, chaotic motions occurred through an infinite number of period-doubling bifurcations.
5. As frequency ratio is changed, the system bifurcates to periodic motions with twice the period of the previous oscillation. One outstanding feature of this scenario is that the critical value of frequency ratio at which successive period doubling occur obey the "Feigenbaum number", after which the motion becomes chaotic.
6. Other diagnostic tools were used to identify chaotic motions of the magnetically levitated vehicle as; fast Fourier transform, Poincaré maps and Lyapunov exponent.
7. Finally the total vibratory characteristics of the system is summarized as a "Chaos Diagram", which indicates the occurrence regions of several types of vibration including chaos, drawn in a parameter plane of frequency and amplitude of the excitation.

REFERENCES

[1] E.H. Gad, "Vibration Analysis of a Rotor-Bearing System Subjected to Nonhomogenous and Parametric Random Excitations", Scientific Bulletin, *Fac. of Eng., Ain Shams Univ.*, Part II, vol. 30, No. 4, p. 203, 1995.

[2] H. Tamura and E.H. Gad, "On Chaotic Behaviours in the Radial Vibrations of a Ball Bearing", *Trans. of JSME* (in Japanese), vol. 58, No. 559, p. 13, C 1992.

[3] R. He and P.G. Vaidya, "Analysis and Synthesis

of Synchronous Periodic and Chaotic Systems", *Phys. Rev.*, A 46, p. 7387, 1992.

[4] H. Tamura and E.H. Gad, "Nonlinear Vibrations in a System having an Asymmetrical Spring with a Single Degree of Freedom", *Proc. of Vibration Conference'93, JSME*, vol. 4, p. 1615, 1993.

[5] H. Tamura, E.H. Gad, and S. Matsubara, "Experimental Study on the Chaotic Motion of a Magnetically Levitated Body", *Proc. of Vibration Conference'93, JSME*, vol. 4, p. 1609, 1993.

[6] B.V. Jayawant, *Electromagnetic Levitation and Suspension Techniques*. Edward Amold, Pub, Ltd, London, 1981.

[7] G.R. Polgreen, "Railway With Magnetic Suspension". *Westinghouse Engineer*, 226, pp. 632-6, 1968.

[8] H. Yabuno, N. Fujimoto, M. Yoshizawa and Y. Tsujioka, "Bouncing and Pitching Oscillations of a Magnetically Levitated Body Due to the Guideway Roughness", *JSME Int. J*, Ser.III, vol. 34, No. 2, p. 192, 1991.

[9] F.C. Moon, *Chaotic and Fractal Dynamics; A Introduction for Applied Scientists an Engineers*, Wiley, New York, 1992.

[10] S.H. Stogatz, *Nonlinear Dynamics and Chao with Applications to Physics, Biology, Chemist and Engineering*, Addison - Wesley Pub. Co New York, 1994.

[11] D. Hobson, "An Efficient Method fo Computing Invariant Manifolds of Plana Maps", *J. Comp. Phys.*, 104, p. 14, 1993.

[12] A. Wolf, et al., "Determining Lyapuno Exponents from a Time Series", *Physica* 16 I p. 285, 1985.

[13] O.H. Yabun, T. Senio, M. Yoshizawa and Y Tsujioka, "Dynamical Behavior of a Levitate Body With Magnetic Guides", *JSME Int. J*, Se 3, vol. 32 No. 3, p. 428, 1988.

[14] J. Yogesh, *Computers Methods for Engineerin* Allyn & Bacon Inc., Boston, 1988.

[15] K. Briggs, "A Precise Calculation of th Feigenbaum Constants", *Mathematics Computation*, 57, p. 435, 1991.